Highly corrupted image inpainting through hypoelliptic diffusion

U. Boscain, R. Chertovskih, J.-P. Gauthier, D. Prandi*, A. Remizov

CMAP, École Polytechnique & LSIS, Université de Toulon

*dario.prn@gmail.com

Abstract

We present an image inpainting algorithm based on hypoelliptic diffusion for the Citti-Petitot- Sarti model of the primary visual cortex V1 [3, 5, 4]. In particular, we focus on the inpainting problem with complete knowledge of the location of the corruption: the damaged image consists of pixels, and we know whether each pixel is damaged or not. Our techniques are an improvement on the semi-discrete approach introduced in [1] for the Citti-Petitot-Sarti model, obtained by introducing heuristic methods that allows for very good reconstructions of highly corrupted images (i.e., with more than 80% of corrupted pixels).

Introduction

In [2, 1] an image reconstruction method based on hypoelliptic diffusion and inspired by the human visual cortex is presented in detail. The crucial neuro-physiological fact behind this model, is that the primary visual cortex V1 lifts a black-and-white image $f : \mathbb{R}^2 \to [0, 1]$ from $\mathbb{R}^2$ to the bundle of directions of the plane $PT\mathbb{R}^2 = \mathbb{R}^2 \times P\mathbb{R}$. Indeed, with some simplifications, neurons of V1 are grouped into orientation columns. Each one of these columns is sensitive to visual stimuli at a given point of the retina $a \in \mathbb{R}^2$ for a given direction $v \in P\mathbb{R}$, independently of its orientation.

Since this algorithm is anthropomorphically inspired, it is not surprising that its performances on highly corrupted images (that the human eye is not able to reconstruct) are less than satisfactory. Here we present some ideas coming from the Petitot-Citti-Sarti model with some heuristic considerations to build an efficient image inpainting algorithm for highly corrupted images. This method is a synthesis of two different approaches to the image reconstruction: the averaging method and the evolutionary method, based on the hypoelliptic diffusion.

Image inpainting through hypoelliptic diffusion

The algorithm developed in [2, 1] operates roughly as follows.

1. **Lift:** The starting image $f(x, y)$ is lifted to the (generalized) function $\bar{f}(x, y, \theta)$ on $PT\mathbb{R}^2$ defined by
$$\bar{f}(x, y, \theta) := \begin{cases} f(x, y), & \text{if } \theta \text{ is the direction of the level set at } f(x, y), \\ 0, & \text{otherwise.} \end{cases} \tag{1}$$

2. **Hypoelliptic evolution:** the space $PT\mathbb{R}^2$, with coordinates $q = (x, y, \theta)$, is endowed with the sub-Riemannian structure with global orthonormal frame given by the two vector fields
$$X_1(q) = \cos\theta \frac{\partial}{\partial x} + \sin\theta \frac{\partial}{\partial y}, \quad X_2(q) = \frac{\partial}{\partial \theta}. \tag{2}$$
The reconstructed function on $PT\mathbb{R}^2$ is then the solution $\psi = \psi(x, y, \theta, t)$ at time $t = 1$ of the initial problem, for $a, b \in \mathbb{R}^2$,
$$\frac{\partial \psi}{\partial t} = \Delta_H \psi, \qquad \psi|_{t=0} = \bar{f}(x, y, \theta). \quad \text{where} \quad \Delta_H := b(X_1)^2 + a(X_2)^2. \tag{3}$$

3. **Projection:** ψ is projected back to a function on $\mathbb{R}^2$, which will be the final result F of the image inpainting procedure, through the formula
$$F(x, y) = \max_{\theta} \psi(x, y, \theta)$$

Dynamic Reconstruction:

The above procedure has the drawback of applying the evolution to the whole image, and thus also on the non-corrupted part, blurring it. In [1], we proposed the following heuristic complement to it, allowing to keep track of the initial information during the evolution. Let the set G of good points be the set of points that are already reconstructed enough (thus including non-corrupted points), and the set B of bad points be the set of points that are still corrupted.

1. Apply the evolution described by (3) for a small time δ;
2. Redefine the values of ψ on G mixing them with the initial values of f. Do not modify ψ on B.
3. Update the sets G and B, promoting to good points those bad points that are "sufficiently well reconstructed".

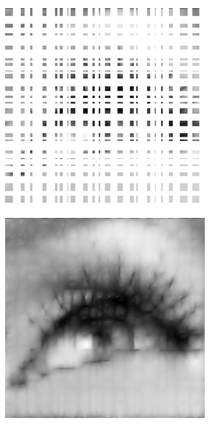

Figure 1: An highly corrupted image reconstructed with the methods from [1].

New algorithm

These surpisingly good results in the reconstruction of highly corrupted images let us to elaborate the following alternative algorithm. Here we mix 2 ideas:

- **Preprocessing phase**: where we fill in a very simple way the corrupted part of the image, to help the lifting procedure and the hypoelliptic diffusion.
- **Modyified hypoelliptic diffusion**: where we substitute the parameters a and b in (3) with functions, aimed at enhancing the diffusion near the corrupted portions of the image and penalizing it elsewhere.

More in detail, the new algorithm is divided in the following 4 steps:

Step 1: Preprocessing phase (Simple averaging)

The aim of this phase is to fill in the corrupted areas of the picture with a rough approximation of what the reconstruction should be, through a discrete approximation of a diffusion. We will call ∂B the set of *boundary bad points*, i.e., of those $(x_k, y_l) \in B$ that are adjacent (horizontally, vertically or diagonally) to some good point. We then iteratively redefine the value of f at each $(x_k, y_k) \in \partial B$ to be the average value of the set G_{kl} of good points in its 9-points neighborhood. After this, we remove (x_k, y_l) from B and add it to G.

Figure 2: Example of step 1 applied to a highly corrupted image.

More precisely, let $f^0 = f$, $G^0 = G$ and $B^0 = B$. Given f^i, G^i and B^i we then define f^{i+1}, G^{i+1} and B^{i+1} as follows. For any $(x_k, y_l) \in \partial B^i$ we put
$$f^{i+1}(x_k, y_l) = \begin{cases} \frac{1}{|G^i_{kl}|} \sum_{(\xi,\eta)\in G^i_{kl}} f^i(\xi, \eta), & \text{if } (x_k, y_l) \in \partial B^i \\ f^i(x_k, y_l) & \text{otherwise.} \end{cases} \tag{4}$$
Observe, in particular, that this formula leaves the values of f^{i+1} on $B^i \setminus \partial B^i$ to be zero. Finally, $G^{i+1} = G^i \cup \partial B^i$ and $B^{i+1} = B^i \setminus \partial B^i$.

Step 2: Main diffusion

In this step we apply hypoelliptic diffusion (3) with varying coefficients $a = a(x, y)$ and $b = b(x, y)$ chosen so that the diffusion is more intensive at the points where the "mosaic" effect, produced by the previous step and visible above, is more strong. Obviously, the diffusion should be as weak as possible elsewhere.

To estimate the intensity of this effect, we use the absolute value of the gradient of the image. Indeed, we apply the hypoelliptic diffusion (3) with lifted initial condition $\bar{f}(x, y, \theta)$, and coefficients $a = a(x, y)$ and $b = b(x, y)$ defined by the following empirical formula, where the parameters a_i, b_i, σ are experimentally chosen,
$$a(x, y) = a_0 + a_1 e^{-\phi^2(x,y)}, \quad b(x, y) = b_0 + b_1 e^{-\phi^2(x,y)}, \quad \text{where } \phi(x, y) = \sigma^{-1}\left(1 - \frac{|\nabla g(x, y)|}{\max |\nabla g|}\right).$$

Step 3: Advanced averaging

After the second step of the algorithm we remove the "mosaic" effect. However, the diffusion introduces a blurring effect, that we cannot remove by decreasing the parameters of the diffusion. We then apply a procedure similar to the first step but guided by the image $h(x, y)$ obtained after the previous step. Namely, the only difference between steps 1 and 3 is that when $(x_k, y_l) \in \partial B^i$, instead than by (4), we define $f^{i+1}(x_k, y_l)$ as
$$f^{i+1}(x_k, y_l) = \arg \min_{X\in[0,1]} \sum_{(\xi,\eta)\in G^i_{kl}} \left| \frac{X}{f^i(\xi, \eta)} - \frac{h(x_k, y_l)}{h(\xi, \eta)} \right|^2. \tag{5}$$
This expression realizes a compromise between the results of step 1 and 2. Moreover, since the expression inside the $\arg\min$ is a continuous convex function in X, the minimum exists and a closed formula solving (5) can be easily derived.

Step 4: Weak smoothing

Since step 3, as step 1, introduces a "mosaic" effect, we essentially repeat step 2. The only difference is that now we use weaker diffusion, the "mosaic" effect gained in step 3 being is much smaller than in step 1.

Figure 3: The image after each step. The second image depicts the modulus of the gradient of the result of step 1, which we use to compute the varying coefficients in step 2.

More results:

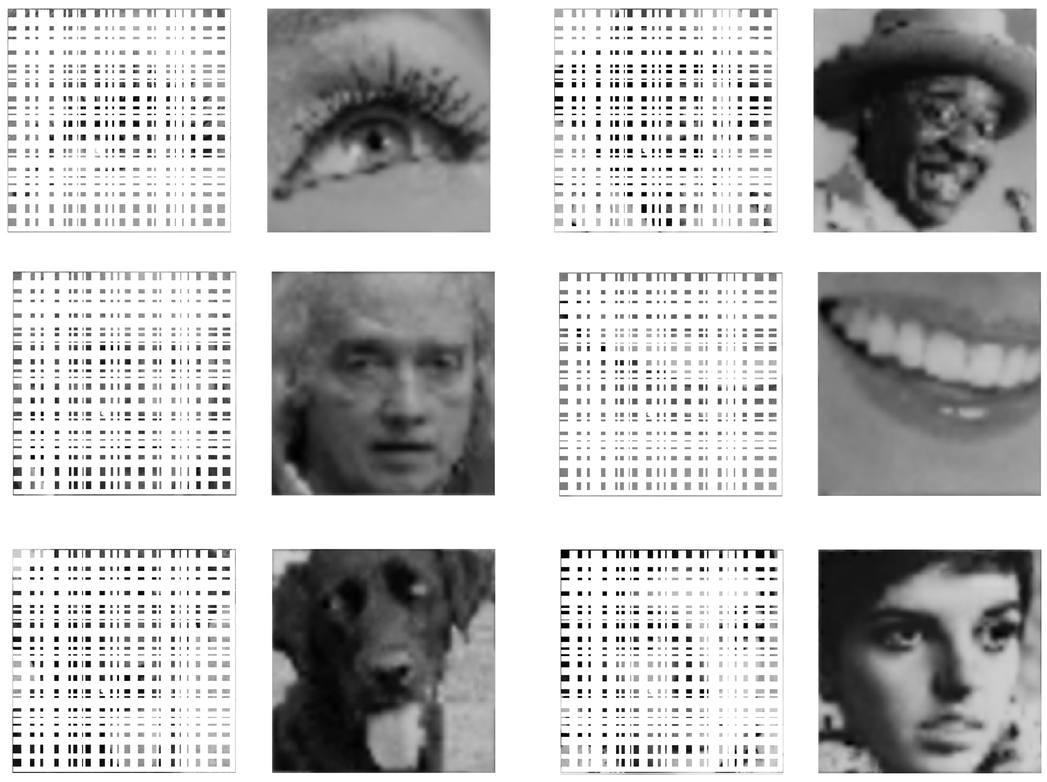

References

[1] U. Boscain, R. A. Chertovskih, J. P. Gauthier, and A. O. Remizov. Hypoelliptic diffusion and human vision: a semidiscrete new twist. *SIAM J. Imaging Sci.*, 7(2):669–695, 2014.

[2] U. Boscain, J. Duplaix, J.-P. Gauthier, and F. Rossi. Anthropomorphic image reconstruction via hypoelliptic diffusion. *SIAM J. Control Optim.*, 50(3):1309–1336, 2012.

[3] G. Citti and A. Sarti. A cortical based model of perceptual completion in the roto-translation space. *J. Math. Imaging Vision*, 24(3):307–326, 2006.

[4] J. Petitot. The neurogeometry of pinwheels as a sub-riemannian contact structure. *Journal of Physiology-Paris*, 97(23):265 – 309, 2003. Neurogeometry and visual perception.

[5] J. Petitot. *Neurogéomètrie de la vision. Modèles mathématiques et physiques des architectures fonctionnelles*. Les Éditions de l'École Polytechnique, 2009.